Synthesis, Electrical, Electronic and Charge Transport Properties of Poly(aniline-co-*p*-toluidine)

Yahya A. Ismail[a]; Afaq Ahmad[b]; Faiz Mohammad[c]
[a] Department of Chemistry, University of Calicut, Kerala, India [b] Department of Chemistry, Aligarh Muslim University, Aligarh, India [c] Department of Applied Chemistry, Aligarh Muslim University, Aligarh, India

PLEASE SCROLL DOWN FOR ARTICLE

Synthesis, Electrical, Electronic and Charge Transport Properties of Poly(aniline-co-*p*-toluidine)

YAHYA A. ISMAIL,[1] AFAQ AHMAD,[2] and FAIZ MOHAMMAD[3]

[1]*Department of Chemistry, University of Calicut, Kerala, India*
[2]*Department of Chemistry, Aligarh Muslim University, Aligarh, India*
[3]*Department of Applied Chemistry, Aligarh Muslim University, Aligarh, India*

Copolymers of aniline with *p*-toluidine were synthesized for different molar ratios of the respective monomers in acid medium. The electrical conductivity, charge transport and spectral characteristics upon incorporation of *p*-toluidine units into the polyaniline backbone were investigated. The electrical conductivity of the copolymers showed frequency dependence which became more prominent with an increase in the number of *p*-toluidine units in the polyaniline backbone. A direct relationship between the frequency dependence and electron localization was observed in the copolymers. Electronic spectra showed blue shifts in the $\pi \rightarrow \pi^*$ and benzenoid $\rightarrow$ quinoid transitions revealing a decrease in the extent of conjugation in the copolymers. The protonated forms of the copolymers were soluble in DMSO giving polaron band around 400 nm. The decrease in electrical conductivity was attributed to the greater electron localizations as revealed from the broader ESR signals. Temperature dependence of electrical conductivity showed that charge transport was mainly through variable range hopping though a mixed conduction behavior was observed at higher temperature range.

1 Introduction

The discovery by the Shirakawa group that doped polyacetylene film could show electrical conductivity as high as 10^3 Scm^{-1} triggered the worldwide research activity in the field of conducting polymers (1). Since then, a number of conducting polymers such as polyaniline (PANI), polypyrrol, polythiophene, polyphenylene etc. were synthesized which showed high electrical conductivity when partially oxidized or reduced (2). Among these, PANI is unique and fascinating because of its high environmental stability, ease of synthesis, moderately high and controllable electrical conductivity and inexpensiveness of the monomer. Moreover, PANI finds its potential in various electrical and electronic applications such as in super capacitors (3) rechargeable batteries (4), biosensors (5), EMI shielding (6), microelectronics (7), artificial muscles and actuators (8), humidity sensors (9), electro chromic display devices (10) and corrosion protection (11). However, poor mechanical stability and processibility of

PANI constitute major obstacles to the extensive applications. For the improvement of mechanical stability and procesibility many strategies like introduction of alkyl, alkoxy, arylhydroxy, amino or halogen groups, preparation of composites and copolymers have been proposed (12–17). The synthesis of copolymers from substituted anilines was found easier and more effective. Although many studies on *o*- and *m*-toluidines based polymers were reported, no such studies have been reported on the synthesis of copolymers derived from *p*-toluidine. Consequently, in this work, poly(aniline-co-*p*-toluidine) was prepared and characterized with an emphasis to study the effect of incorporation of *p*-toluidine on the resulting copolymers.

2 Experimental

2.1 Materials and Synthesis

Aniline (Ranbaxy Chemicals) and *o*-methylaniline (*o*-toluidine) (E. Merk, India) were double distilled prior to use. *p*-methylaniline (*p*-toluidine) (99%, Sisco Chemicals) was recrystallized from alcohol and then from acetone while potassium persulphate (99%, CDH Chemicals, AR), hydrochloric acid (Merck India, AR) and ammonia

Address correspondence to: Yahya A. Ismail, Department of Chemistry, University of Calicut, Kerala, India 673635. Tel.: +91-494-2401144 Ext. 413; Fax: +91-494-2400269; E-mail: aiyahya123@gmail.com

(CDH Chemicals, AR) were used as received. Spectroscopic grade solvents were used for recording the UV-VIS spectra.

PANI and copolymers for different molar ratios of aniline and *p*-toluidine were synthesized chemically using potassium persulphate ($K_2S_2O_8$) as oxidant under acidic conditions (18). In a typical procedure, aniline and *p*-toluidine (0.01 mol. each) dissolved in 100 ml of 1 M HCl were reacted with $K_2S_2O_8$ (0.025 mol) dissolved in 150 ml of 1 M HCl at $26 \pm 2°C$ with constant stirring for 6 h. The dark colored viscous reaction mixture was filtered. The product was washed with triple-distilled water several times to remove the excess of oxidant and HCl until the filtrate became neutral. The product then was washed with methanol followed by acetone to remove low molecular weight oligomers, vacuum dried at $50°C$ in an air oven. The product was treated with 0.25 M NH_4OH solution to prepare the corresponding base from. The copolymer was labeled as P(APT)1:1. Copolymers for 1:2 and 1:3 molar ratios of aniline and *p*-toluidine were also synthesized to obtain P(APT)1:2 and P(APT)1:3, respectively. A copolymer of aniline with *o*-toluidine for 1:1 molar ratio, P(AOT)1:1 was also synthesized by similar procedure.

2.2 Characterization

The UV-VIS spectra were recorded at room temperature using a UV-VIS Spectrophotometer (Elico, SL 151, India). FTIR spectra were recorded in KBr pellets using a FTIR Spectrophotometer (Schimadzu, 8101-A, Japan) at room temperature. For measuring the electrical conductivity, the polymers were finely powdered and made into pellets using a stainless steel die of 1.326 cm^2 cross-sectional area and by applying a pressure of 4 tons using a hydraulic press (Spectra Lab, India). The pellets were placed between two polished platinum electrodes mounted on a stainless steel sample holder assembly between copper leads which were electrically insulated from the sample holder by teflon sheets. The electrical conductivity was measured by a two-probe method using a RLC Digibridge (Genrad 1659 RLC Digibridge, USA) at two different frequencies, viz. 100 Hz and 10 KHz. The temperature dependence of electrical conductivity was studied from room temperature up to $180°C$ at 10 KHz by keeping the cell containing the pellets in an air oven and maintaining a heating rate of $1°C/\text{min}$. To study the basic nature of charge transport, the temperature dependence of conductivity data was fitted to Variable Range Hopping model (19). ESR spectra were recorded on a GEOL ESR Spectrometer (JES-RE2X, Japan) at room temperature under the following settings: modulation frequency: 100 KHz, microwave frequency: 9.44 GHz, microwave power: 5 mV, scan range: 300 G, field modulation 10 G, time constant 0.035 and center field: 3350 G. The 'g' values, peak to peak line widths (ΔH_{pp}) and line asymmetry parameter (a/b ratios) were estimated from the ESR spectra.

Table 1. % Yield and time taken for the initial color change of the reaction mixture

Polymer	% Yield	Time taken for the initial color change of the reaction mixture (min.)
PANI	80.03	1–2
P(AOT)1:1	70.1	3–4
P(APT)1:1	49.84	10–12
P(APT)1:2	41.73	14–16
P(APT)1:3	25.4	17–20

3 Results and Discussion

3.1 Polymer Synthesis

The copolymerization of aniline with *o*- and *p*-toluidines were found to be a slow process compared with the homopolymerization of aniline to form PANI. The appearance of a greenish color in the reaction mixture was taken as the indication of copolymerization. The time taken for the initial color change of the reaction mixtures upon addition of the oxidant along with the % yield of the polymers are given in Table 1. It is clear that the rate of reaction decreased as the ratio of *p*-toluidine increased in the reaction mixture. It is a qualitative indication that in presence of toluidine units, the aniline monomers alone could not homopolymerize, rather the toluidine units were incorporated in the polymer backbone. The observed decrease in the rate of polymerization can be explained on the basis of steric effect of methyl groups, which is more pronounced in the copolymerization of aniline with *p*-toluidine. The anilinium cation radical produced first during the polymerization can exist in three canonical structures as shown in Figure 1 (20). The corresponding cation radicals produced in *o*-toluidine and *p*-toluidine may be shown as in Figures 2 and 3, respectively.

In the copolymerization of aniline with *o*-toluidine, we expect a normal linear polymer by the coupling of N-radical cation 1, with the para-radical cation 5, which suffers a
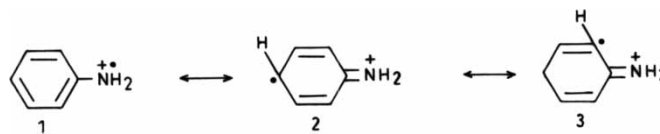

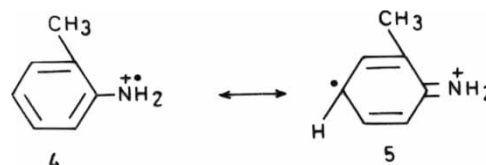**Fig. 1.** Canonical structures of anilinium cation radical of aniline.

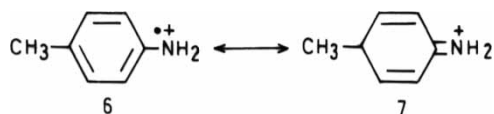**Fig. 2.** Cation radical produced in *o*-toluidine.

Fig. 3. Cation radical produced in *p*-toluidine.

comparatively lesser steric effect than that suffers during the polymerization of aniline with *p*-toluidine. Here, since the para-positions are already blocked, coupling should take place at the ortho-position to -NH$_2$ group. It is clear from Figure 3 that, for the formation of copolymer of aniline with *p*-toluidine, the N-radical cation of aniline 1, should couple with the radical cation of *p*-toluidine 7, which experiences a much greater steric effect. Also, the steric effect increases as the ratio of *p*-toluidine units increases in the reaction mixture. This describes the difference in the rate of copolymerization reactions. A comparatively poor yield of the copolymers of aniline with *p*-toluidine may be a qualitative indication that the copolymers are of lower chain length and the copolymerization process may get easily terminated. It was observed that the solubility of the resulting copolymers increased as the ratio of *p*-toluidine was increased as shown in Table 2.

3.2 FTIR Spectral Studies

The FTIR spectra of PANI and the copolymers are shown in Figures 4 and 5 and the corresponding absorptions are presented in Table 3 The spectrum of PANI has two major absorptions at 1589.6 cm^{-1} and 1492.4 cm^{-1} due to the C=C vibrations of benzenoid and quinoid units, respectively (21–23). The number of quinoid units is almost equal to the number of benzenoid units in PANI as there was no apparent difference in the relative intensity of quinoid to benzenoid band which is a measure of the degree of the oxidation of the polymer chain (23). The band appeared at 1299 cm^{-1} is due to C-N stretching vibrations of benzenoid–quinoid–benzenoid sequence (23). The strong band at 1125 cm^{-1} is the characteristic band of the charged defects (24, 25).
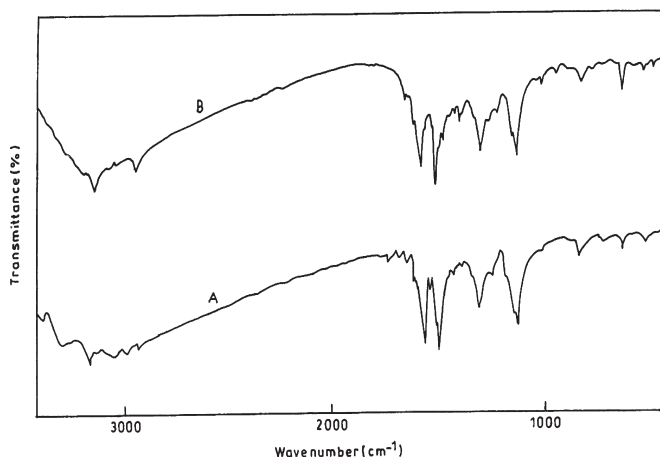

Fig. 4. FTIR Spectra of (A) PANI and (B) P(AOT)1:1.

The weak bands at 3300 cm^{-1} are due to N-H stretching vibrations. In the FTIR spectrum of P(AOT)1:1, the relative intensity of quinoid band is slightly less than that of benzenoid band which is suggestive of the lower oxidation state of the copolymer. The band at 1124.5 cm^{-1} and 1293 cm^{-1} correspond to charged defects and C-N stretching vibrations, respectively. Unlike the spectra of polyaniline, the band observed at 1385 cm^{-1} is due to C-H bending vibrations of -CH$_3$ groups. The bands between 890–1112.6 cm^{-1} are attributed to 1,2,4-tri-substitution of the benzene ring and ascribed to the C-H out of plane and in plane bending modes (26). The weak band at ∼2950 cm^{-1} is attributed to -C-H stretching vibrations of methyl group.

As seen from Figure 4, in the FTIR spectra of all the copolymers of aniline with *p*-toluidine, the C=C benzenoid vibrations occur at 1582.47 cm^{-1}, 1579.56 cm^{-1} and at 1567.7 cm^{-1} and the quinoid vibrations occur at 1504 cm^{-1}, 1501.9 cm^{-1} and 1505.5 cm^{-1}, respectively for P(APT)1:1, P(APT)1:2 and P(APT)1:3. Comparatively weaker bands observed around ∼1405 in P(APT)1:1, ∼1406 cm^{-1} in P(APT)1:2 and at 1403 cm^{-1} in P(APT)1:3 may be attributed to -C-H bending vibrations of -CH$_3$ groups. The band observed

Table 2. Solubility characteristics of the polymers in various solvents at room temperature (≈25 ± 2)°C

Polymer	As-prepared protonated form					Base form				
	H$_2$O	H$_2$SO$_4$	Acetone	DMF	DMSO	H$_2$O	H$_2$SO$_4$	Acetone	DMF	DMSO
PANI	IS	MS	IS	IS	IS	IS	SS	IS	MS	MS
P(AOT)1:1	IS	S	IS	SS	MS	IS	S	SS	S	S
P(APT)1:1	IS	S	SS	S	MS	IS	S	MS	S	S
P(APT)1:2	IS	S	MS	S	S	IS	S	MS	S	S
P(APT)1:3	IS	S	S	S	S	IS	S	S	S	S

IS − Insoluble.
MS − Moderately soluble.
SS − Slightly soluble.
S − Soluble.
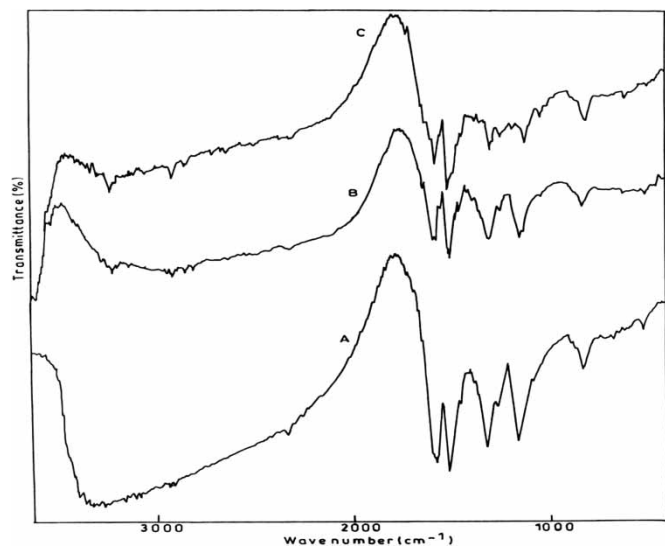
Fig. 5. FTIR spectra of (A) P(APT)1:1 (B) P(APT)1:2 and (C) P(APT)1:3.

Fig. 6. UV-VIS spectra of the base form of (A) P(AOT)1:1 and (B) P(APT)1:1 in DMSO.

at 1310.8 cm^{-1} in P(APT)1:1 and at 1301.44 cm^{-1} in P(APT)1:2 and at 1287 cm^{-1} in P(APT)1:3 are attributed to C-N stretching vibrations. This absorption shifted to lower frequencies as the ratio of *p*-toluidine increases in the copolymer composition. The bands around 1240 cm^{-1} are due to charged defects. The bands at ∼815 cm^{-1} and the multiple bands between ∼1014 cm^{-1}−1046 cm^{-1} in all the copolymers are attributed to 1,2,4 tri-substitution of the benzene ring.

3.3 Electronic Spectral Studies

UV-VIS absorption spectra of the base form of P(AOT)1:1 and P(APT)1:1 in DMSO are shown in Figure 6 and that of P(APT)1:2 and P(APT)1:3 are shown in Figure 7. The UV-VIS spectra of the as-prepared protonated form of the copolymers of aniline with *p*-toluidine taken in DMSO and H$_2$SO$_4$ are presented in Figures 8 and 9, respectively. The corresponding absorption peak positions are presented in
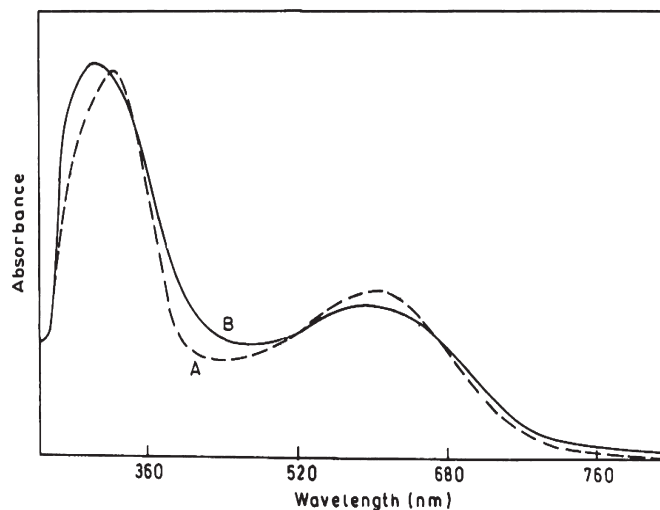
Table 4. It can be seen from Figures 6 and 7 that, the copolymers showed two major absorptions corresponding to $\pi \to \pi^*$ transition at higher energy side, which is a measure of the extent of conjugation between the adjacent phenyl rings and benzenoid to quinoid exciton transitions at lower energy side (27, 28). There is a hypsochromic shift in both the absorption bands of the copolymers as compared to that in polyaniline. The shift is more prominent in copolymers derived from *p*-toluidine. It is clear from Table 4 that, the blue shift increases as the ratio of the *p*-toluidine units increases in the copolymer.

When methyl groups are present on the phenyl rings, they substantially alter the planarity of the system and influence the π-orbital overlap resulting in a shift in the $\pi \to \pi^*$ transition band. Thus, the blue shift was due to the presence of a methyl group present in the phenyl ring which ultimately resulted in the increase of band gap of the copolymers (29). The planarity of the phenyl rings seems to be affected to a greater extent in the copolymers of aniline with *p*-toluidine.

Table 3. Characteristic FTIR absorption frequencies (wave number, cm^{-1}) of the as-prepared copolymers

| PANI	P(AOT)1:1	P(APT)1:1	P(APT)1:2	P(APT)1:3	Band characteristics
3254	3250	3300	3248	3239	N-H Stretching vibration
—	2956	2973	2931	2925	C-H Stretching vibrations due to CH$_3$
1589.6	1583.4	1582.47	1579.56	1567.7	C=C Benzenoid vibration
1496	1515.5	1504	15.2	1505	C=C Quinonoid vibration
—	1386	1405	1406	1403	C-H Bending of CH$_3$ groups
1299	1296	1310.8	1301.4	1287	C-N Stretching vibration
1248	1256	1240	1238	1236	Vibration due to charged defects
—	1007	1015	1038	1046	1,2,4 Tri substitution
—	890	860	874	865	Tri substitution of phenyl ring due to CH$_3$ group
825	821	819	809	813	*p*-di Substitution of aromatic ring
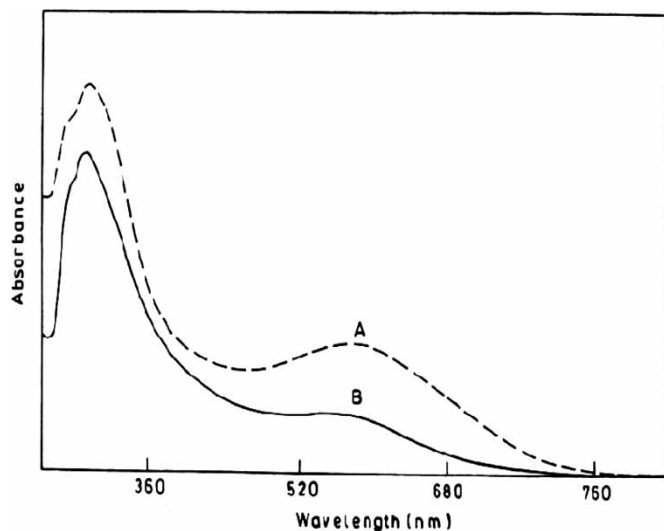
Fig. 7. UV-VIS spectra of the base form of (A) P(APT)1:2 and (B) P(APT)1:3 in DMSO.

The exciton band produced by the inter/intra-chain charge transfer is due to an absorption from the highest occupied molecular orbital (HOMO) band centered on the benzenoid units to the lowest unoccupied molecular orbital (LUMO) band centered on the quinoid units. This band is a measure of the extended conjugation (29, 30). The blue shift observed for this band is explained in terms of an increase in the ring torsional angle between the adjacent phenyl ring caused by the steric effect due to the presence of methyl groups on the ring. The greater the steric effect, the greater will be the extent of blue shift. Copolymers of aniline with
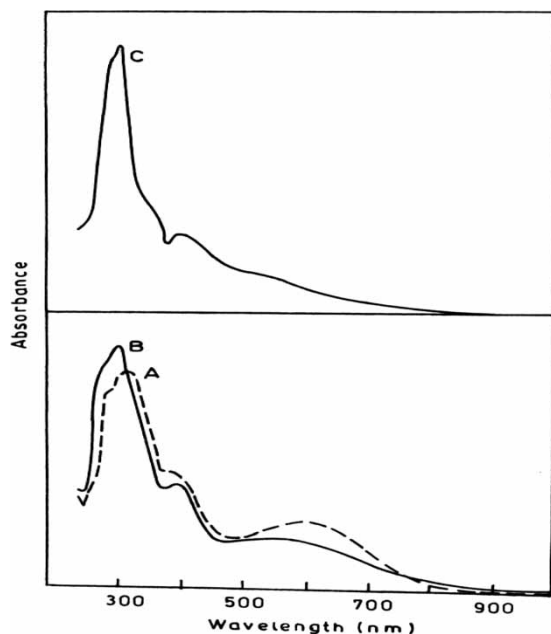

Fig. 8. UV-VIS spectra of protonated forms of (A) P(APT)1:1 (B) P(APT)1:2 and (C) P(APT)1:3 in DMSO.
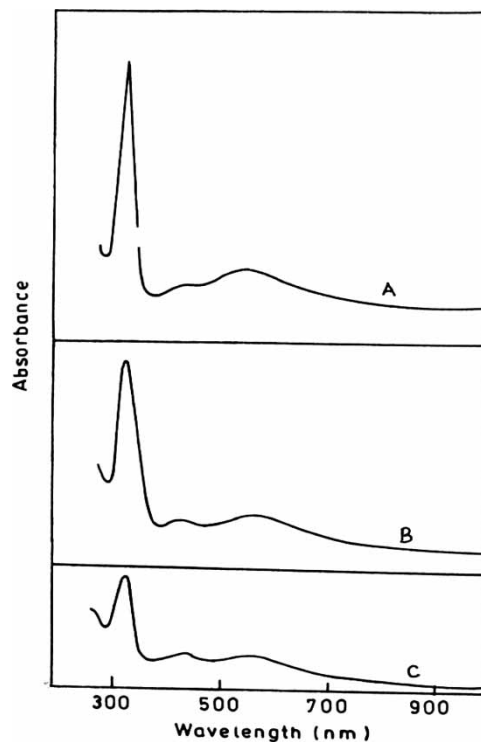

Fig. 9. UV-VIS spectra of protonated forms of (A) P(APT)1:1 (B) P(APT)1:2 and (C) P(APT)1:3 in H_2SO_4.

p-toluidine suffered a greater steric effect caused by the *p*-toluidine units. The relative intensity of the exciton band is a measure of the degree of oxidation of the polymer chain (30). Therefore, it can also be concluded that, the oxidation state of the copolymers decreases as the ratio of *p*-toluidine increases in the copolymers. This supports the findings from FTIR spectra as explained earlier.

As seen from Figure 8, UV-VIS spectra of as-prepared protonated forms of the copolymers derived from *p*-toluidine in DMSO showed peaks around 410 nm due to the polaron transitions (30−32). But the broad band around 800 nm, generally observed for protonated forms of polyanilines and poly(o-toluidine) as observed by Kulkarni et al. (32) was not

Table 4. UV-VIS peak positions (nm) of base forms and protonated forms of the polymers in DMSO and DMF

Polymer	Base form		Protonated form	
	DMSO	DMF	DMSO	H_2SO_4
PANI	325, 626	326, 620	—	—
P(AOT)1:1	320, 598	321, 596	—	—
P(APT)1:1	300, 590	290, 579	300, 406, 605	320, 430, 571
P(APT)1:2	291, 581	287, 572	299, 409, 571	319, 428, 572
P(APT)1:3	280, 570	278, 567	290, 411, 535	320, 425, 571

observed in our copolymers. The blue shift observed for this band increases with an increase in the molar ratio of *p*-toluidine. Figure 9 showed the bands corresponding to $\pi \to \pi^*$ transition, polaron transition and benzenoid to quinoid exciton transition when the spectra were recorded in H_2SO_4. But here we did not observe any apparent shift in the $\pi \to \pi^*$ transition and benzenoid to quinoid transition bands, though there was a blue shift in the absorption band corresponding to polaron transition. As can be seen from Table 4, the base form, as well as the protonated forms of copolymers, showed solvatochromism when the spectra were recorded in DMF, DMSO and H_2SO_4.

3.4 ESR Spectral Studies

The ESR spectral parameters such as 'g' value, peak to peak line width ΔH_{pp} and line asymmetry a/b ratio of the polymers along with their electrical conductivities are summarized in Table 5. The area under ESR signal is related to the number of spins present in the sample and the width of the signal may be related to the extent of delocalization of electrons and thus to the extent of conjugation. The position of ESR signal may be related to the neighboring environment of electronic spin, the 'g' factor (33, 34). The symmetry of ESR signals and spin-lattice relaxation time can be interpreted in terms of the electrical conduction theories in conducting polymers (35). It can be seen from Table 5 that, the 'g' value and ΔH_{pp} gradually increases with decreases in the electrical conductivity of the polymers, where as a/b ratio increases with increase in electrical conductivity. 'g' value and ΔH_{pp} are minimum for PANI and maximum for P(APT)1:3. These observations are consistent with some of the earlier reports that, narrow line width is suggestive of longer conjugation length and greatly delocalized electronic spin gives narrow ESR signals (33, 34), though there are some different opinions (36). When substituents are present in the phenyl rings as in the case of copolymers studied here, they tend to localize the electronic spin and have lower conjugation length resulting in comparatively higher 'g' value and ΔH_{pp} and smaller a/b ratio. Therefore, it can be concluded from the ESR data that, electron localization in the polymers increases as the ratio of *p*-toluidine increases in the polymers chain affecting their electrical conductivity. Electron localization increases in the order,

PANI < P(AOT) 1:1 < P(APT) 1:1 < P(APT) < 1:2 < P(APT)1:3.

3.5 Electrical Conductivity and Charge Transport Studies

The two probe electrical conductivity measured at frequencies of 100 Hz and 10 KHz are presented in Table 5. The results of the variation of electrical conductivity with temperature studied in the temperature range of 25−180°C for P(AOT)1:1 and P(APT)1:1 fitted in Arrhenius equation (Band Model) and variable range hopping (VRH) model are shown in Figures 10 and 11. It can be seen from Table 5 that the copolymers showed lower electrical conductivity than polyaniline. The electrical conductivity measured at 10 Hz was found to be greater than that measured at 100 Hz. The frequency dependence was more prominent in copolymers of aniline with *p*-toluidine and it increased with the increase of *p*-toluidine content in the copolymers backbone.

Though the electron donating alkyl group makes the electronic flow along a single polymer chain a little better, the observed decrease in the electrical conductivity of the copolymers may then be explained in terms of the decreased extent of conjugation and an increase in the band gap caused by increased phenyl ring tortional angles resulted from the steric repulsion between the adjacent phenyl rings due to the presence of $-CH_3$ groups (29, 37). The copolymers of aniline with *p*-toluidine experience a greater steric repulsion and a larger decrease in the extent of conjugation, thereby a larger increase in the band gap causing a greater reduction in electrical conductivity. The above factors may result in greater electron localization. As the ratio of *p*-toluidine increases in the copolymer backbone, electron localization also increases. These findings are supported by electronic spectral studies and ESR studies. There is also a possibility of decreased inter-chain diffusion of charge carriers in the copolymers induced by the increased separation of the polymer chains due the presence of $-CH_3$ groups and hence a reduced coherence between the polymer chains (38).

One of the fascinating observations of our studies is the frequency dependence of electrical conductivities of the copolymers. The electrical conductivity measured at 10 Hz was greater than that measured at 100 Hz. The frequency

Table 5. Electrical conductivity and ESR data

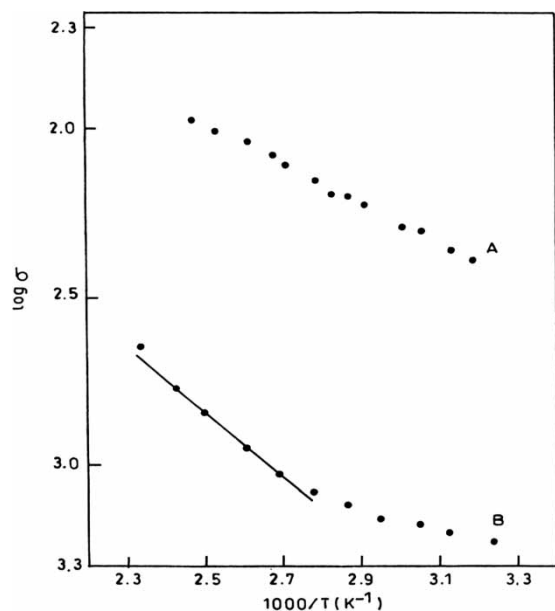| Polymer | Electrical conductivity (Scm^{-1}) | | ESR Data | | |
	100 Hz	10 KHz	'g' Value	ΔH_{pp} (G)	a/b Ratio
PANI	7.167×10^{-1}	7.168×10^{-1}	2.013	13.04	1.60
P(AOT)1:1	5.3×10^{-3}	5.342×10^{-3}	2.02	14.47	1.47
P(APT)1:1	5.71×10^{-4}	6.76×10^{-4}	2.022	15.61	1.41
P(APT)1:2	1.64×10^{-5}	8.57×10^{-5}	2.026	16.32	1.37
P(APT)1:3	6.46×10^{-8}	1.05×10^{-6}	2.032	17.93	1.30

Fig. 10. Arrhenius plot of log σ vs. $1000/T$ (K^{-1}) for (A) P(AOT)1:1 and (B) P(APT)1:1.

dependence was more prominent in copolymers of aniline with *p*-toluidine and it increased gradually with an increase in the ratio of *p*-toluidine in the copolymers. Greater localization of charges leads to reduced conductivity and substituent causes an increase in the disorder (39). It was clear from our studies that, the greater the electron localization, the greater is the frequency dependence. Frequency dependence of electrical conductivity gradually increases in the copolymers
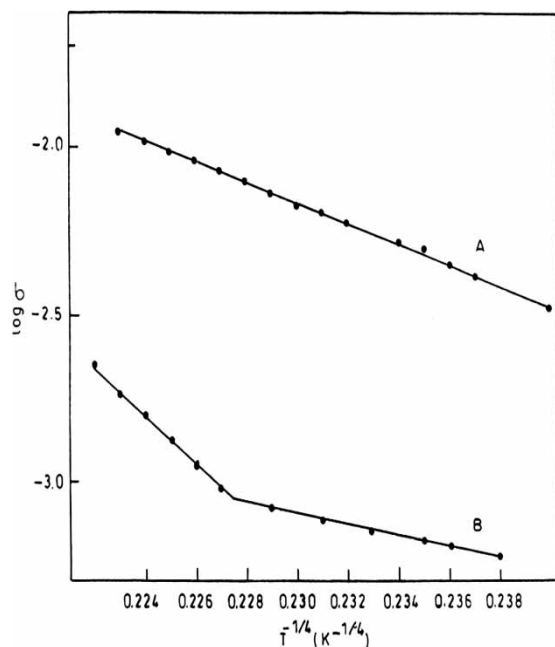

Fig. 11. Plot of log σ vs. $T^{-1/4}$ $(K^{-1/4})$ corresponding to VRH model for (A) P(AOT)1:1 and (B) P(APT)1:1.

of aniline with *p*-toluidine with the increase in the ratio of *p*-toluidine because of a gradual increase of electron localization which is consistent with ESR results.

The temperature dependent electrical conductivity studies revealed a thermally activated conduction phenomena in both P(AOT)1:1 and P(APT)1:1. The electrical conductivity increases linearly with increase in temperature in the whole of the temperature range studied. The conductivity was not affected by moisture or humidity though it was reported that presence of moisture affects the electrical conductivity of polyaniline (40). The loss of moisture leading to increased localization of electrons and thereby a reduction in electrical conductivity was not operative in these polymers. This may be an indication that, static defects such as chain ends and chemical defects control the charge transport in these copolymers.

The observed electrical conductivity - temperature data was found to fit best in the equation corresponding to variable range hopping model (40).

$$\sigma\,(T) = \sigma_0 \exp\left(\frac{T_0}{T}\right)^{1/4}$$

where T_0 is the Mott's characteristic temperature and σ_0 is the electrical conductivity at room temperature. Comparing Figures 10 and 11, it is clear that a variable range model can be used to explain the conduction phenomena in P(AOT)1:1 over the entire range of temperature studied. In P(APT)1:1 also, the VRH model is applicable up to 93°C after which it followed the same equations but with a change of slope.

In the higher temperature range (90−150°C), it seems that the charge transport follows band conduction (Arrhenius model) in (PAP)T 1:1 as the electrical conductivity − temperature data fit best in the equation,

$$\sigma\,(T) = \sigma_0 \exp\left(-\frac{E_A}{kT}\right)$$

where E_A is the energy of activation and k is the Boltzmznn constant.

4   Conclusions

p-Toluidine units could be incorporated in PANI backbone through chemical polymerization of respective monomers. As the ratio of *p*-toluidine increases, the oxidation state of the copolymer was decreased. The blue shift in the UV-VIS absorption bands and the lower electrical conductivity of copolymers were due to the decrease in the extend of conjugation and an increase in the torsional angle between adjacent phenyl rings due to steric strain caused by -CH$_3$ groups. The electrical conductivity decreased as the ratio of *p*-toluidine was increased in the copolymers. But the frequency dependence of electrical conductivity increased with the increase of *p*-toluidine units due to greater electron localization as

revealed from the ESR studies. Where as variable range hopping model could be used to explain the charge transport in P(AOT)1:1 a mixed conduction mechanism was operative in P(APT)1:1 in the temperature range of $25-150°C$.

5 Acknowledgments

The authors would like to thank the Heads of the Departments of Chemistry and Applied Chemistry, AMU, Aligarh for providing the necessary facilities for the successful completion of this work. The help rendered by Prof. R.J. Singh, Dept. of Physics, AMU, Aligarh for carrying out the ESR experiments is greatly acknowledged.

6 References

1. Shirakawa, H., Louis, E.J., MacDiarmid, A.G., Chiang, C.K. and Heeger, A.J. (1977) *J. Chem. Soc. Chem. Commun.*, 578−580.
2. MacDiarmid, A.G. (2002) *Synth. Met.*, **125**, 11−22.
3. Wang, Y.G., Li, H.Q. and Xia, Y.Y. (2006) *Adv. Mater.*, **18**, 2619−2623.
4. Karami, H., Mousavi, M.F. and Shamsipur, M. (2007) *J. Power Sour.*, **164**, 896−904.
5. Gerard, M. and Malhotra, B.D. (2005) *Curr. Appl. Phys.*, **5**, 174−177.
6. Niu, Y. (2006) *Polym. Comp.*, **27**, 627−632.
7. Gupta, R.K. and Singh, R.A. (2005) *J. Polym. Res.*, **11**, 269−276.
8. Smela, E. and Mattes, B.R. (2005) *Synth. Met.*, **151**, 43−48.
9. Kulkani, M.V., Vishwanath, A.K., Aiyer, R.C. and Khanna, P.K. (2005) *J. Polym. Sci., B: Polym. Phys.*, **43**, 2161−2169.
10. Talaie, A., Lee, J.Y., Lee, Y.K., Jang, J., Romagnoli, J.A., Taguchi, T. and Maeden, E. (2000) *Thin Solid Film*, **363**, 163−166.
11. Lu, W.K., Elsenbaumer, R. and Wessling, B. (1995) *Synth. Met.*, **71**, 2163−2166.
12. Dhawan, S.K. and Trivedi, D.C. (1992) Electrochem. Soc. Extended Abstract No 682.
13. Wei, Y., Focke, W.W., Wnek, G.E., Ray, A. and MacDiarmid, A.G. (1989) *J. Phys. Chem.*, **93**, 495−499.
14. Dhawan, S.K. and Trivedi, D.C. (1993) *Synth. Met.*, **60**, 67−71.
15. Barole, D.D., Kapadi, U.R., Mahulikar, P.P. and Hundiwale, D.G. (2006) *Designed Monomer Polymer*, **9**, 349−357−370.
16. Gok, A. and Sari, B. (2002) *J. Appl. Polym. Sci.*, **84**, 1993.
17. Savitha, P. and Sathyanarayana, D.N. (2004) *Polym. Int.*, **53**, 106−112.
18. Yahya, A.I., Ahmad, A. and Mohammad, F. (2004) *Ind. J. Chem. A*, **43**, 1423−1428.
19. Mzenda, V.M., Goodman, S.A. and Auret, F.D. (2002) *Synth. Met.*, **127**, 285−289.
20. Oshima, N.T. and Yan, H. (1995) *Bull. Chem. Soc. Japan*, **68**, 1056−1063.
21. Roy, B.C., Gupta, M.D. and Ray, J.K. (1995) *Macromolecules*, **28**, 1727−1732.
22. Genies, E.M. and Noel, P. (1990) *J. Electroanal. Chem.*, **296**, 473−490.
23. Trivedi, D.C. In *Handbook of Organic Conductive Molecules Polymers*; Nalwa, H.S. (ed.); John Wiley & Sons, Vol. 2, p. 537, 1997.
24. Shackelette, L.W., Wolf, J.F., Gould, S. and Baughman, R.H. (1988) *J. Chem. Phys.*, **88**, 3955−3961.
25. Challier, T. and Slade, R.C.T. (1994) *J. Mat. Chem.*, **4**, 367−372.
26. Chiang, J.C. and MacDiarmid, A.G. (1986) *Synth. Met.*, **13**, 193−205.
27. Epstein, A.J., Ginder, J.M., Zuo, F., Bigelow, W.R., Woo, W.S., Tanner, D.B., Ritcher, A.F., Huang, W.S. and MacDiarmid, A.G. (1987) *Synth. Met.*, **18**, 303−309.
28. Stafstrom, S., Bredas, J.L., Epstein, A.J., Woo, H.S., Tanner, D.B., Huang, W.S. and MacDiarmid, A.G. (1987) *Phys. Rev. Lett.*, **59**, 1464−1467.
29. Yue, J., Wang, Z.H., Cromaek, K.R., Epstein, A.J. and MacDiarmid, A.G. (1991) *J. Am. Chem. Soc.*, **113**, 2665−2671.
30. Zagorska, M., Adam, P. and Lefrant, S. In *Handbook of Organic Conductive Molecules and Polymers*; Nalwa, H.S. (ed.); John Wiley & Sons, Vol. 3, p. 194, 1997.
31. Ahmad, N., Feng, F., Schursky, H. and Shah, S. (1993) *Ind. J. Chem., A*, **32**, 679−684.
32. Kulkarni, M.V., Viswanath, A.K. and Khanna, P.K. (2006) *J. Macromoecular Sci., Part A, Pure and Applied Chemistry*, **43**, 197−203.
33. Mohammad, F., Calvert, P.D. and Billingham, N.C. (1995) *J. Phys. D. Appl. Phys.*, **28**, 1−6.
34. Langer, J.J., Krzyminiewzki, R., Kruczynski, Z., Gibnski, T., Czajkowski, I. and Framski, G. (2001) *Synth. Met.*, **122**, 359−362.
35. Poole, C.P. *Electron Spin Resonance: A Comprehensive Treatise on Experimental Techniques*; Wiley: New York, 1982.
36. Choi, K.M., Kim, K.H. and Choi, J.S. (1989) *J. Phy. Chem. Solids*, **50**, 283−290.
37. Umare, S.S., Borkar, A.D. and Gupta, M.C. (2002) *Bull. Mat. Sci.*, **25**, 235−240.
38. Wang, Z.H., Javadi, H.H.S., Epstein, A.J., Ray, A. and MacDiarmid, A.G. (1990) *Phys. Rev. B*, **42**, 54115414.
39. Pinto, N.J., Shah, P.D., Kahol, P.K. and McCormick, B.K. (1996) *Solid State Commun.*, **97**, 1029−1031.
40. Mzenda, V.M., Goodman, S.A., Auret, F.D. and Prinsloo, L.C. (2002) *Synth. Met.*, **127**, 279−283.